

STRESS RELAXATION CRACKING (SRC) SUSCEPTIBILITY COMPARISON IN UNS S34709 AND UNS S34751 STAINLESS STEEL WELDS FOR PETROCHEMICAL PIPING APPLICATIONS

Tim Pickle¹, Jean Fuenmayor², Jorge Penso³, Zhenzhen Yu¹

¹Colorado School of Mines, Golden, CO, USA

²Shell Norco Energy and Chemicals Park, Norco, Louisiana, USA

³Shell Global Solutions (US) Inc., Houston, Texas, USA

ABSTRACT

UNS S34751 and UNS S34709 austenitic stainless-steel alloys contain thermomechanical properties required for use in chemical processing pipe applications with 900-1200°F (482-665°C) operating temperatures. UNS S34751 alloy has demonstrated improved sensitization resistance compared to UNS S34709, a precursor for polythionic acid stress corrosion cracking (PA-SCC), due to lower carbon (C) content (0.01 wt.%) and higher niobium-to-carbon (Nb/C) ratio with lower overall niobium content. The addition of nitrogen (N) in UNS S34751 alloy provides similar thermomechanical properties compared to UNS 34709. Additionally, stress relaxation cracking (SRC) susceptibility in UNS 34709 welds has been documented thoroughly in literature and industry, which poses a problem for long term service life, while UNS S34751 welds have potential for improved SRC resistance without the need for post weld heat treatment (PWHT). In this paper, a literature review of S34751 is explored, and testing matrix of experimental SRC tests using a Gleeble 3500® thermomechanical simulator is developed for S34751 gas tungsten arc welded (GTAW) pipe samples in comparison to S34709 welds. Additionally, initial thermodynamic and kinetic CALPHAD calculations have been completed to analyze potential detrimental phases in S34751 in comparison to S34709, e.g., γ -phase. SRC testing has been mostly completed in S34709 welds made with W34710 (E347-16) and S16880 (E16.8.2-15) weld filler, respectively, and SRC comparisons to S34751 are in progress. Current results show higher resistance to SRC in S34751 HAZ and FZ than S34709 FZ and W34710 FZ at 800°C. In the following year, a full comparative analysis between S34709 and S34751 HAZ and FZ, in addition to welds with alternative filler S16880, is planned, including SRC testing at 600-750°C temperatures, metallurgical

characterization of intergranular and intragranular precipitates, and additional thermodynamic analyses to complement microstructural observations. Final conclusions on SRC susceptibility comparisons between S34751 and S34709 welds, including alternative fillers, will be made.

Keywords: austenitic stainless steel, polythionic acid stress corrosion cracking, stress relaxation cracking, weldability

NOMENCLATURE

ASTM	American society for testing and materials
BCC	body-centered cubic
BM	base metal
CALPHAD	CALculation of PHase Diagrams
δ	delta ferrite
FCC	face-centered cubic
FZ	fusion zone
γ	gamma austenite
GTAW	gas tungsten arc welding
HAZ	heat affected zone
IPM	inches per minute
LOM	light optical microscopy
MTR	material test report
PA-SCC	polythionic acid stress corrosion cracking
PFZ	precipitate free zone
PRISMA	precipitation module
PWHT	post weld heat treatment
RT	room temperature
SEM	scanning electron microscopy
SRC	stress relaxation cracking
TTT	time-temperature-transformation
UNS	unified numbering system

1. INTRODUCTION

The refining industry requires the use of elevated temperature and corrosion resistant tubular alloys for charge heater furnaces in delayed coking processing. To combat low and elevated temperature corrosion mechanisms in charge heaters, a move from 9Cr-1Mo ferritic alloys to austenitic stainless steels is economically significant by increasing the time span between decoking procedures, thereby becoming economically significant since coking in the charge heaters is the limiting factor in charge rates and unit run lengths. Additionally, the decoking process typically causes increases in the tube temperatures of 200°F above normal operating condition to 1300°F (704°C) from 1100°F (593°C), but creep is expected to be negligible during decoking in contrast to service operating conditions. Overall, thermally stable austenitic stainless steels could offer both metallurgical and economic advantages.

Stress relaxation cracking (SRC) has been recognized as a significant concern affecting the longevity (e.g., months to years) of industries operating at elevated temperatures, such as oil and gas chemical processing pipe applications and renewable energy concentrating solar power applications [1-3]. The main factors contributing to SRC are a combination of tensile residual or external stresses, elevated temperatures, and susceptible microstructures (e.g., precipitate free zones) [4]. In highly restrained welds or pipe bends with enough tensile stress, the time to fracture at elevated temperatures above 500°C (932°C) can be within months to a few years [5]. Various techniques have been used to perform SRC evaluation on different alloys, including three-point bend tests [2] and uniaxial thermomechanical test methods [6-10]. A three-point bend testing at 600°C showed cracks in the S34709 sample weld without PWHT but not in S34751[11]. Another study tested at SRC susceptibility in a load frame by first applying a weld HAZ simulation, followed by application of 20% strain at RT, heating up to temperature of 650°C without restriction, and then applying 5% strain at temperature followed by holding test at constant strain and up to 300 hours [12]. The results show that S34751 lasted the whole 300 hours while the S34709 sample failed within 3 hours. It was also reported that S34751 has better SRC resistance than S34709 without post weld heat treatment [13].

UNS S34751, an alloy with lower carbon (C) (~0.01 wt%), added nitrogen (N) content (0.08wt%), and lower niobium (Nb) content (~0.3 wt%), as tabulated in Table 1, may provide more resistance to SRC and polythionic acid-stress corrosion cracking (PA-SCC) [14-17] than UNS 34709 due to its less potential for grain boundary chromium (Cr)-rich $M_{23}C_6$ and NbC [12]. Alloys susceptible to PA-SCC, a different mechanism from SRC, would be identified with the presence of a sensitized microstructure, i.e., depletion of elemental Cr on grain boundaries and Cr carbide grain boundary precipitation, or ditching of grain boundaries using oxalic acid grain boundary etching using ASTM A262 standard after thousands of hours of exposure at service temperatures [14]. In contrast to PA-SCC, intergranular SRC may be evident without the presence of a sensitized microstructure, but with the presence of a NbC precipitate free

zone (PFZ), a leading hypothesis for SRC in S34709 welds [18]. A higher niobium-to-carbon (Nb/C) ratio and lower C content improves the resistance to formation of grain boundary Nb rich MX carbides and reduces Cr-rich $M_{23}C_6$, as seen in S34751 alloy after aging at 700°C for 24 hours [14], which would reduce sensitization and susceptibility to PA-SCC. Also, higher Nb/C ratios could help prevent the severity of strain aging due to predictably less volume fraction of bulk NbC, which contributes to the SRC mechanism. Further work is needed to evaluate whether an increase in nitrogen (N) in UNS 34751 would contribute to formation of Cr and Nb nitrides (CrNbN), such as z-phase [19], that may be detrimental for SRC. Additionally, an excessive amount of sulfur impurity may contribute to grain boundary decohesion by reducing grain boundary surface energy as it substitutionally diffuses to grain boundaries or cracks under stress, while phosphorous and tin was reported to have negligible impact on brittle intergranular failure [20]. S34751 is designed to contain lower sulfur content compared to S34709.

For S34709 welds, the susceptibility to SRC is higher than most S3XXXX alloys, and PWHT was needed to eliminate SRC in S34709 welds [2, 11]. Recent work on studying S34709 welds have shown relatively high susceptibility to cracking in both HAZ and FZ that is dependent on plastic strains, initial residual stress and temperature [6, 9]. The use of alternative weld filler S16880 in S34709 welds instead of matching filler (W34710) contributes to improved toughness and improved elevated temperature ductility at PWHT temperatures of 1600°F (899°C) [7]. Diffusion based phase transformation of sigma phase seemed to correlate with depreciated toughness in matching filler after elevated temperature exposure, due to more initial as-welded δ-ferrite in W34710 FZ than S16880 FZ [7]. Recent work has also shown beneficial creep properties of S16880 in elevated temperatures (750-825°C) with respect to S31609, but S16880 has potentially concerning low creep life at 650°C due to the formation of isothermal ferrite [21]. While using S16880 rather than matching W34710 may be relatively beneficial, determining long-term SRC susceptibility and correlated phase transformations at service temperatures in S16880 welds in comparison to W34710 is critical for weld design.

In this study, SRC in pipe welds of S34751 with matching filler is evaluated to understand the impact of temperature, stresses, and strains on time-to-fracture in S34751 welds using a Gleeble 3500® thermomechanical simulator. In the following year, SRC test results in pipe welds of S34751 using alternative S16880 filler will be presented. Results will be compared to S34709 welds, with matching (W34710) and alternative (S16880) filler, respectively, at both elevated temperatures >1382°F (750°C) and furnace temperatures of 930-1300°F (499-704°C). Metallurgical characterizations and CALPHAD equilibrium and kinetic calculations will be implemented to supplement the SRC results.

2. MATERIALS AND METHODS

2.1 Material compositions

The compositions of S34709 and S34751 are shown in Table 1 below, obtained from material test reports (MTRs). The

main composition differences between the two materials are C, N, and Nb levels. S34751 contains lower C, higher N, and lower Nb levels than S34709. However, S34751 contains a higher Nb/C ratio, and has a minimum ratio specification of 15, while S34709 has a Nb/ratio minimum specification of 8.

TABLE 1: Alloying chemical compositions of S34709 substrate, W34710 matching filler to S34709, S16880 alternative filler, S34751 wrought pipe, and S34751 matching filler.

Elem.	S34709 Spec.	S34709 Exp.	W3 471 0	S1 68 80	S34751 Spec.	S34751 Exp.	S34751 weld filler
Cr	17-19	17.3	19.5	16	17-19	17.2	19.1
Ni	9-13	9.1	10.1	8.5	9-13	9.8	8.3
Mn	2 max	1.0	1.5	1.7 8	0-2	1.54	1.62
							8X
Nb	(C+N)- 1 max	0.58	0.36	-	0.2-0.5	0.3	0.41
Mo	-	0.32	0.2	1.1 7	-	0.36	0.35
Co	-	-	-	-	-	0.33	0.31
Cu	-	0.21	0.16	0.0 8	-	0.08	0.07
Si	0.75 max	0.51	0.54	0.2 2	0.1-0.5	0.4	0.38
C	0.04- 0.1	0.05	0.03	0.0 41	0.005- 0.02	0.012	0.03
N	-	0.03	0.03	0.0 3	0.07- 0.1	0.08	0.13
P	0.045 max	0.029	0.02	0.0 22	0.03 max	0.026	0.002
S	0.03 max	0.002	0.01	0.0 08	0.01 max	0.001	0.001
Nb/C	≥8	11.6		≥15	25		

2.2 Thermodynamic CALPHAD calculations

Equilibrium and kinetic calculations are conducted using Thermo-Calc steels and F-alloys software package, including TCFE13 and MOBFE7 databases. The equilibrium and precipitation calculators (PRISMA) are used to generate equilibrium single axis diagrams and time-temperature-transformation (TTT) curves to indicate time-at-temperature effects on phase transformations at service-related temperature ranges.

2.3 Welding Procedure

Half-inch thick S34751 seamless pipes with a 4.5-inch (114 mm) outer diameter are circumferentially multi-pass welded using gas-tungsten arc welding (GTAW) using a single-V weld geometry with a 70° groove angle, as seen in Figure 1 (a). The welding parameters in the filler region are within a range of 150-180 Amps and a travel speed range of 2.8-6 IPM using a weaving pattern. The arc energy per unit length ranges from 21.5-40 kJ/in depending on the weld layer and travel speed. The root pass is 27 kJ/in, followed by a hot pass of 40 kJ/in. The subsequent passes then have a heat input on average less than 30 kJ/in in the half-inch thick tube.

2.4 SRC test sample extraction plan, Gleeble 3500® test procedure, and experimental plan

The sample extraction plan and tensile sample geometry can be seen in Figure 1 (a-b) and (c), respectively. Three types of samples are machined parallel to the axial direction of the pipe or transverse to the circumferential weld. The first type (Type 1) of samples is centered on the weld fusion zone (10 samples), the second type (4 samples) is centered on the weld HAZ/FZ boundary (Type 2), and sample three (10 samples) is in the unaffected base metal (Type 3). Type 1 sample tests crack susceptibility in the FZ, Type 2 sample tests actual weld HAZ susceptibility, and Type 3 sample will be used to physically simulate a weld HAZ and be compared to Type 2 sample test results.

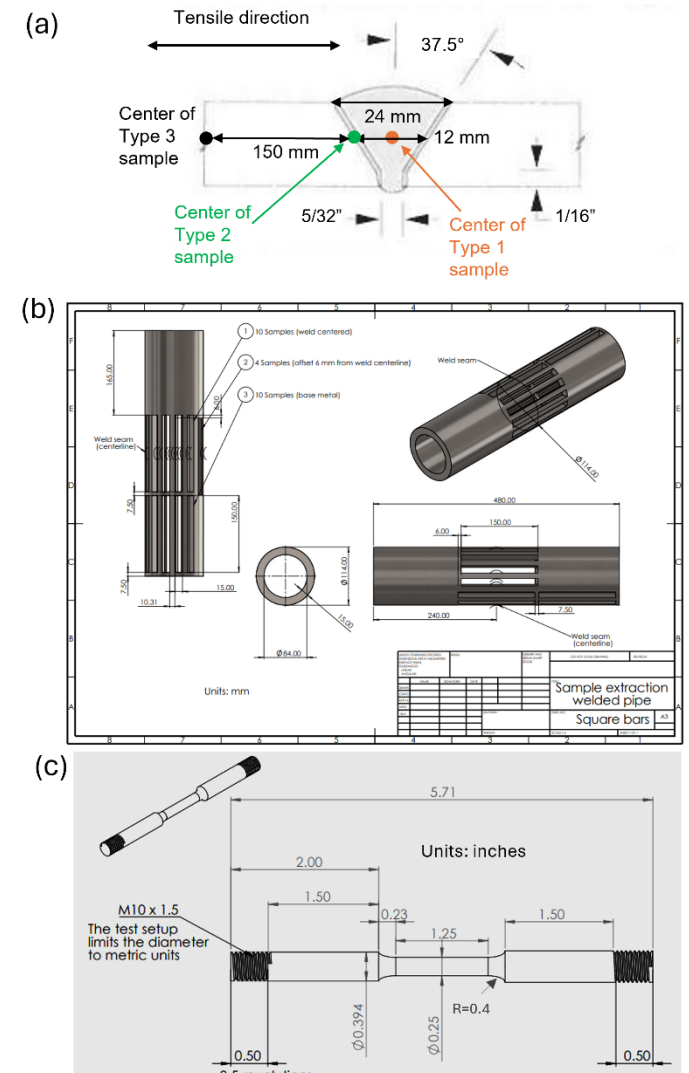


FIGURE 1: (a) Weld joint geometry overlaid with center locations of the three types of samples (FZ (Type 1), HAZ (Type 2), and BM (Type 3)), (b) weld sample extraction plan for S34751 pipes, and (c) sample geometry of sample used for Gleeble® 3500 tests.

The SRC test is conducted using a Gleeble 3500® thermomechanical physical simulator, with an example test procedure shown in Figure 2. The test procedure involves four steps for physically simulated HAZ specimens or three steps for pipe weld extracted HAZ and FZ samples, with details described in another publication [9]. Figure 1 illustrates the experimental procedure for physically simulated HAZ including: 1) applying a thermal cycle for HAZ simulation with fast heating and cooling rates, 2) applying external stresses representative of residual stresses and strains, 3) heating up to test temperature while under stress, and 4) constraining displacement and hold at temperature for a 22-24-hour time-period. If samples do not fail, they are either air cooled under constraint or pulled to fracture to quantify fracture strain. The latter case in the last step is to determine temperature and initial stress/strain effects on ductility. Since the test time at temperature may be too short for cracking to occur in S34751 samples in contrast to S34709 samples, capturing thermomechanical data at the last step (if no fracture happens during stress relaxation) would be a quantifiable tool to compare cracking susceptibility. For pipe weld extracted HAZ and FZ samples, the first step of applying a thermal cycle is excluded.

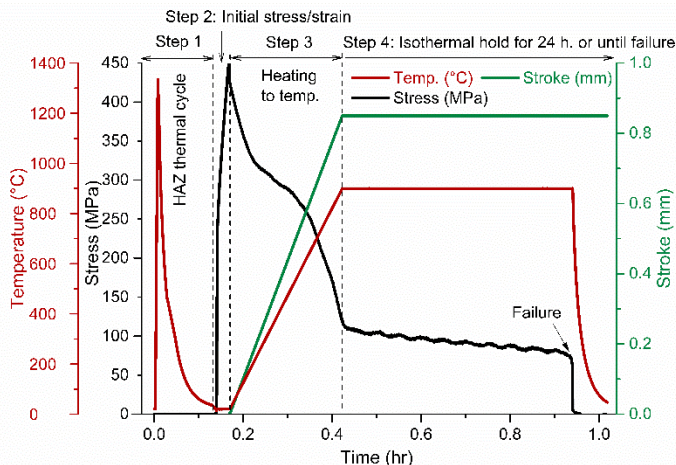


FIGURE 2: Experimental four-step SRC test procedure for simulated HAZ samples. Pipe weld extracted samples do not require Step 1.

The test temperature of interest for the S34751 samples pertains to service temperatures, which ranges from roughly 500-704°C. A slightly higher temperature range of 600-800°C is the optimal temperature range to test for SRC using at least two stress and strain conditions representing extreme (17% strain/600 MPa) and more representative (10% strain/450 MPa) cases, as seen in modeling work on 347H SS welds [22]. Table 2 includes the experimental plan of the S34571 weld FZ samples and HAZ samples. While most samples will be tested in the as-welded condition, the effects of service aging time and temperature (e.g., 600°C for 1000 hours) on microstructure may be conducted followed by stress relaxation testing to compare to as-welded condition.

Additionally, the planned tests on S34571 will be compared to S34709, including three conditions: 1) physically simulated

HAZ, 2) cross-weld samples centered on FZ with matching W34710 filler, and 3) cross-weld samples centered on FZ with alternative S16880 filler. The variables tested for these samples include starting stress of 150-600 MPa and test temperatures 750-1050°C.

TABLE 2: Experimental plan of S34751 samples as starting stress vs. temperature. The planned test time at temperature will be a minimum of 22 hours(h).

Material	Temperature (°C)	Initial Stress/Strain	Planned test time
S34751 FZ (Sample #1)	800	~400-420 initial stress (estimated yield strength)	22 h min.
	750		
	700		
	650		
	600		
	800	600 MPa (extreme case with additional plastic strain)	22 h min.
	750		
S34571 HAZ (sample #2 and 3)	800	17% initial strain (extreme case)	22 h min.
	750		
	700		
	650		
	600		
	800	10% initial strain (more representative of real case)	22 h min
	750		
	700		
	650		
	600		

2.5 Metallurgical characterization procedures

Two sets of samples are investigated and characterized using both light optical microscopy (LOM) and scanning electron microscopy (SEM) methods to analyze the grain size and morphology and phases present. The first set of samples is the as-welded samples, and the second set of samples is SRC tested samples. Additionally, fractography is planned to be performed on second set of samples to analyze the fracture surfaces and determine if SRC fracture characteristics are present, such as intergranular cracks.

3. RESULTS AND DISCUSSION

3.1 CALPHAD Simulations

Figure 3 shows the thermodynamic simulation results of equilibrium phases in S34709 and S34751 base metals. The main secondary phases within a primary γ austenite matrix (FCC L12

crystal structure) are δ ferrite (BCC A2), Nb (C, N) precipitates, z-phase precipitates (CrNbN rich), and various intermetallic phases, including sigma (σ) phase (Fe and Cr-rich intermetallic), eta (η) phase (CrNiSiMo intermetallic), Laves phase (Fe_2Nb), and G-phase. S34751 contains higher nitrogen content (2-3 times that of S34709) at the expense of lower C (~0.01 wt%), which contributes to a tendency for z-phase to form at a wide temperature range of 500-1250°C. A review on z-phase in 9-12 Cr wt% steels (e.g., Gr 91 steel) showed diffusion based phase transformations, likely due to dissolution of MX carbonitrides, over the course of thousands of hours between temperatures of 600-700°C [19].

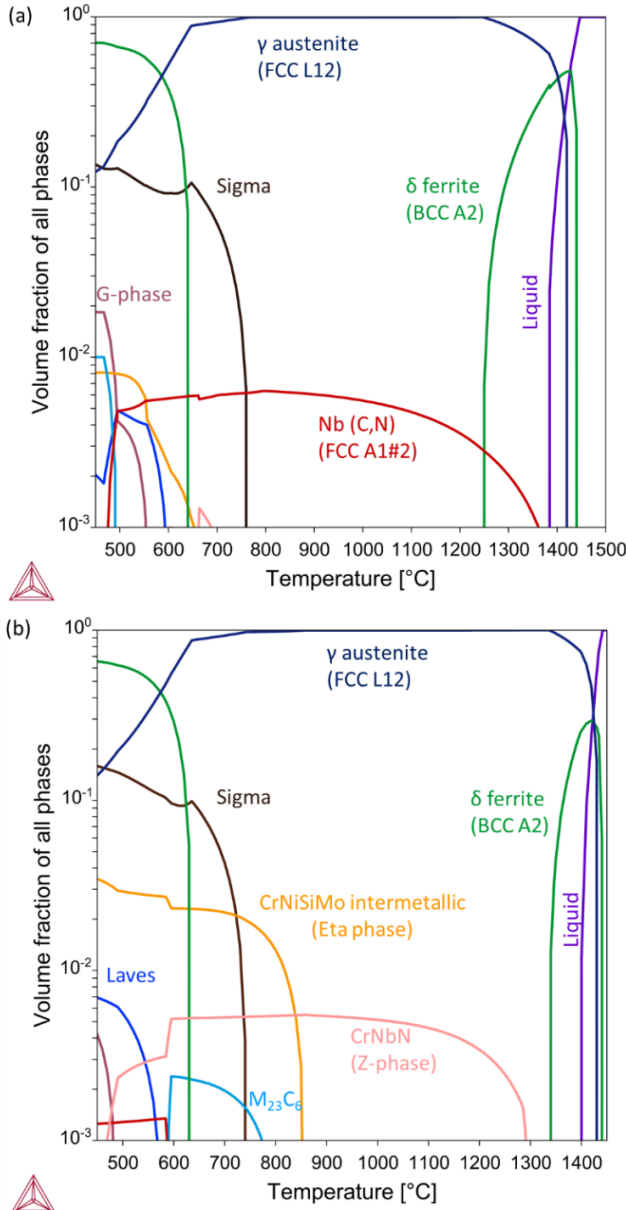


FIGURE 3: CALPHAD thermodynamic single axis equilibrium diagrams showing volume fraction of phases as a function of temperature in (a) S34709 and (b) S34751 base microstructures

The kinetic diagrams based on S34751 composition in Figure 4 show the z-phase can develop quickly at elevated temperatures and form most actively at 950°C. As shown in recent literature, S34751 samples that have been SRC tested up to 300 hours at 650°C exhibited some intragranular z-phase and precipitates, but very little grain boundary phases were present [12]. The effects of service aging time and temperature conditions on microstructure and SRC susceptibility will be analyzed.

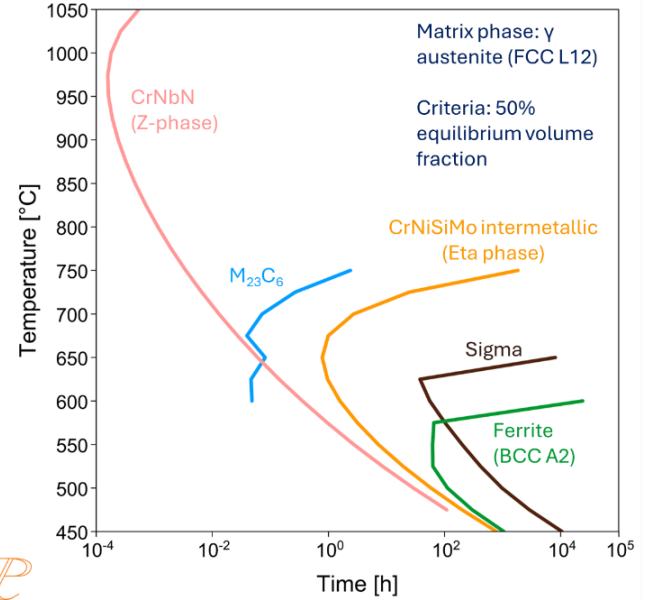


FIGURE 4: CALPHAD TTT diagrams of bulk secondary phases in S34751 base microstructure with γ -austenite being the matrix phase and with a stop criterion of 50% equilibrium volume fraction

3.2 SRC results of S34709 welds

The SRC results of S34709 plate welds, including physically simulated HAZ, matching filler FZ (W34710), and alternative filler FZ (S16880) are summarized in Figure 5. It shows a failure maps representing starting stress at room temperature (representative of residual stresses) as a function of testing temperature for three sets of data, which includes some data referenced by the same authors [9]. For each set of data, particularly the HAZ and matching filler FZ, samples either failed within a 24-hour period at temperature (fail at T), failure upon air cooling (fail on C) or did not exhibit failure (no failure). For all the cross-welded samples with a matching filler and with gauge section centered on the weld FZ, failure occurred within the FZ. The matching filler FZ (W34710) of S34709 welds performs worse than the physically simulated HAZ of S34709 welds. The alternative filler S16880 performed the best since failure never occurred in the FZ. Instead, any failures that occurred in welds made with alternative filler occurred in the adjacent HAZ of S34709 or W34710 material (repair weld case). The S34709 HAZ has been reported to be susceptible to cracking at service type temperatures in multiple literature reports [2, 23].

24]. Additional testing (shaded region in Figure 5) will be performed for UNS S34709 welds at lower, furnace operating service temperatures (600-750°C) to enable a comprehensive and systematic comparison to alloy S34751 stress relaxation tests as planned in Table 2.

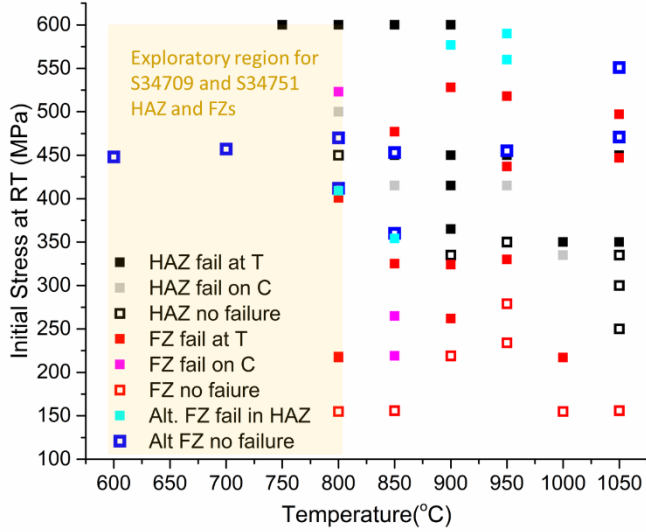


FIGURE 5: Failure map as a function of starting stress and test temperature for S34709 HAZ, matching filler FZ (W34710), and alternative FZ (S16880). Failure is categorized as failure at temperature within a 24-hour period (fail at T), failure upon air cooling (fail on C), or no failure. Alternative FZ (S16880) samples did not fail ever in FZ, but rather in the HAZ of S34709 adjacent to the weld center.

3.3 SRC results of S34751 welds

For this section, SRC testing of S34751 welds is in progress and a full comparison will be made with S34709 results. The full results are anticipated to be completed within a couple of months based on the experimental plan.

Initial experiments have been conducted on S34751 physically simulated HAZ with 17% initial strain and cross-welded S34751 pipe sample with 400 MPa initial stress at 800°C. The comparison to the S34709 counterpart samples is illustrated in Figure 6(a) for physically simulated HAZ (Type 3) and Figure 6(b) for cross-welded FZ (Type 1). Based on these initial tests, S34751 HAZ fails at temperature at roughly seven hours, while the cross-welded W34751 sample did not fail within a 24-hour period at temperature. In contrast, the S34709 HAZ failed within 3.5 hours at temperature, while the W34710 FZ (matching filler for S34709) failed within 0.25 hours at temperature. These initial results indicate higher SRC resistance in the S34751 HAZ and W34751 FZ compared to S34709 HAZ and W34710 FZ. The continued testing results, particularly at temperatures closer to service conditions, will confirm if S34751 alloy would be a more viable option than S34709 alloy with respect to cracking susceptibility.

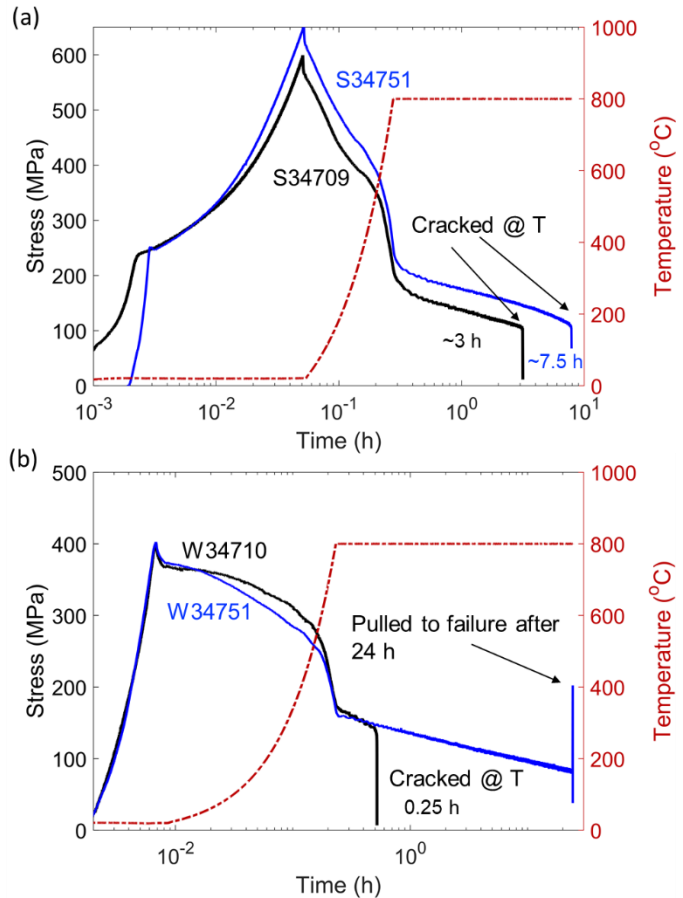


FIGURE 6: SRC test results: (a) comparison between S34709 and S34751 physically simulated HAZ (Type 3) at 800°C with initial strain of 0.174 and stress of ~600 MPa. S34751 failed at approximately 7.5 hours at temperature while S34709 failed at around 3 hours at temperature; and (b) comparison between W34710 and W34751 cross welded FZ samples (Type 3) with initial stress of 400 MPa and test temperature of 800°C. W34751 endured a 24-hour test at 800°C, while the W34710 failed at approximately 0.25 hours at temperature.

4. CONCLUSION

The use of UNS S34751 alloy for charge heater components in delayed coking processes has been of interest in the petrochemical industry. SRC may occur within months to years in various precipitation hardened stainless steel welds, particularly UNS S34709. UNS S34751, a relatively lower C alloy with higher Nb/C ratio and higher N content, may be less susceptible to SRC than UNS 34709. Initial SRC results on UNS 34709 showed high susceptibility in the FZ of welds with a matching W34710 filler, while alternative S16880 filler reduces SRC susceptibility and failure shifts to the S34709 HAZ. S34751 physically simulated HAZ and pipe cross-welded W34751 FZ samples demonstrate higher resistance to SRC than S34709 HAZ and W34710 FZ at 800°C. Further testing of both S34751 FZ and

HAZ at service temperatures is of interest to verify the improved SRC resistance of S34751 pipe welds in comparison to S34709 welds.

5. FUTURE PLAN

The work necessary to provide a comprehensive assessment of the SRC comparison between UNS 34709 and 34751 is:

- Gleeble 3500® thermomechanical testing of UNS S34751 and S34709 HAZ and W34710, W34751, and S16880 FZ at a temperature range of 600-750°C.
- Metallurgical characterization and fractography of UNS S34751 SRC samples and comparison to UNS 34709 is planned for additional funding period.

ACKNOWLEDGEMENTS

This work is financially supported by the Manufacturing & Materials Joining Innovation Center (Ma²JIC), an industry and university cooperative research center (IUCRC) partially funded by the National Science Foundation (NSF) with award No. 2052819.

REFERENCES

[1] H. van Wortel, "Control of Relaxation Cracking in Austenitic High Temperature Components," presented at the NACE Corrosion, Nashville, TN, 2007.

[2] E. C. Dillingh, A. Bahrami, and A. P. Aulbers, "Stress Relaxation Cracking-Augmented Recommended Practice," TNO report, 2016.

[3] C. E. v. d. Westhuizen, "Stress Relaxation Cracking of Welded Joints in Thick Sections of a TP347 Stabilized Grade of Stainless Steel," presented at the Corrosion 2008.

[4] A. Dhooge, "Survey on reheat cracking in austenitic stainless steels and Ni base alloys," *Welding in the World*, vol. 41, pp. 206-219, 1998.

[5] R. D. Thomas, Jr., "HAZ Cracking in Thick Section of Austenitic Stainless Steels-Part 2," *Welding Journal*, vol. 63, pp. 355-368, 1984.

[6] R. Kant and J. N. DuPont, "Stress Relief Cracking Susceptibility in High-Temperature Alloys," *Welding Journal*, vol. 98, pp. 29-49, 2019.

[7] C. Fink, H. Wang, B. T. Alexandrov, and J. Penso, "Filler Metal 16-8-2 for Structural Welds on 304H and 347H Stainless Steels for High Temperature Service," *Welding Journal*, vol. 99, pp. 312-322, 2020.

[8] C. Sarich, B. Alexandrov, A. Benatar, and J. Penso, "Test for stress relief cracking susceptibility in creep resistant chromium-molybdenum steels," *Science and Technology of Welding and Joining*, vol. 27, pp. 265-281, 2022.

[9] T. Pickle, Y. Hong, J. Vidal, C. Augustine, and Z. Yu, "Stress relaxation cracking susceptibility evaluation in 347H stainless steel welds," *Welding in the World*, 2024.

[10] K. Strader, B. T. Alexandrov, and J. C. Lippold, "Stress-Relief Cracking in Simulated-Coarse-Grained Heat Affected Zone of a Creep-Resistant Steel," in *Cracking Phenomena in Welds IV*, ed: Springer, 2016, pp. 475-493.

[11] J. van der Veer, "Three Stress Relaxation Cracking Tests on Cold Deformed Base Materials 347H in As-Delivered Condition and after PWHT and 347 AP in As-Delivered Condition," TNO2014.

[12] T. Osuki, Y. Suzuki, S. Kurihara, T. Ono, and M. Ueyema, "Proposal of 18Cr-8Ni based Austenitic Stainless Steel with Superior Stress Relaxation Cracking Resistance," in *Association for Materials Production and Performance (AMPP)*, San Antonio, TX, 2022.

[13] T. Osuki, M. Seto, H. Okada, M. Sagara, S. Matsumoto, and T. Ono, "Development of Fit-for-Purpose Austenitic Stainless steels with High Polythionic Acid Stress corrosion Resistance," presented at the ASME 2017 Pressure Vessels and Piping Conference, Waikoloa, Hawaii, 2017.

[14] S. A. Bradley, M. W. Mucek, H. Anada, and T. Osuki, "Alloy for resistance to polythionic acid stress corrosion cracking for hydroprocessing applications," *Materials & Design*, vol. 110, pp. 296-303, 2016.

[15] X. Guo, W. Gao, K. Chen, Z. Shen, and L. Zhang, "Corrosion and Stress Corrosion Cracking Susceptibility of Type 347H Stainless Steel in Supercritical Water," *Corrosion*, vol. 74, pp. 83-95, 2017.

[16] T. Osuki, K. Ogawa, Y. Suzuki, S. Kurihara, A. Seki, and M. Ueyema, "Polythionic Acid Stress Corrosion Cracking On Proprietary UNS S34751," presented at the CORROSION 2021, Virtual, 2021.

[17] T. Osuki, Y. Suzuki, K. Yamada, and T. Ono, "Effect of Carbon Content on Polythionic Acid Stress Corrosion Cracking Resistance for UNS S34751 with Extra Low Carbon Content," presented at the CORROSION 2019, Nashville, Tennessee, 2019.

[18] J. Siebert, J. Shingledecker, and T. Lolla, "Stress Relaxation Cracking (SRxC) and Strain Induced Precipitation Hardening (SIPH) Failures," in *DOE Workshop: Evaluation of Welding Issues in High Nickel and Stainless Steel Alloys for Advanced Energy Systems*, 2020.

[19] H. K. Danielsen, "Review of Z phase precipitation in 9-12wt-Cr steels," *Materials Science and Technology*, vol. 32, pp. 126-137, 2016.

[20] S. R. Ortner and C. A. Hippsley, "High temperature brittle intergranular failure in austenitic stainless steels," *Materials Science and Technology*, vol. 8, pp. 883-895, 1992.

[21] O. DeNonno, J. F. Gonzales, S. Tate, R. Hamlin, and J. Klemm-Toole, "Role of Austenite Stability in Elevated Temperature Mechanical Properties of Gas Metal Arc-

Directed Energy Deposition Austenitic Stainless Steels," *JOM*, 2024.

[22] Y. U. Hong, T. Pickle, J. Vidal, C. Augustine, and Z. Yu, "Impact of Plate Thickness and Joint Geometry on Residual Stresses in 347H Stainless Steel Welds," *Welding Journal*, vol. 102, pp. 279-292, 2023.

[23] R. D. Thomas, Jr. and R. W. Messler, "Welding Type 347 Stainless Steel-An Interpretive Report," *Welding Research Council Bulletin*, vol. Bulletin 421, 1997.

[24] N. Morishige, M. Kurabayashi, N. Okabayashi, and T. Naiki, "On the Prevention of Service Failure in Type 347 Stainless Steel," presented at the Third International Symposium of the Japan Welding Society, 1978.